Electronic Supplementary Material (ESI) for Materials Advances.

Thermoelectric characterization of crystalline nano-patterned silicon membranes.

Hafsa Ikzibane[a], Akash Patil[a,b], Jon Canosa[a], Etienne Okada[a], Etienne Blandre[a], Emmanuel Dubois[a] and Jean-François Robillard[a,*]

[a.] *Univ. Lille, CNRS, Centrale Lille, Junia, Univ. Polytechnique Hauts-de-France, UMR 8520 - IEMN – Institut d'Electronique de Microélectronique et de*
[b.] *Nanotechnologie, F-59000 Lille, France STMicroelectronics - 850 rue jean Monnet 38920 Crolles (France)*
[c.] ** jean-francois.robillard@iemn.fr*

Supplementary Materials

1. Seebeck coefficient measurement Device:

The Seebeck coefficient measurement device for silicon (Si) thermoelectric material includes a suspended Si membrane connected to two gold (Au) metallic pads for measuring Seebeck voltage created due to temperature difference. Four pads linked to platinum heaters/sensors enable modeling of the heat source through the Joule effect and measurement of temperature variations, ensuring the absence of current leakage. The five metallic pads, with dimensions of 100 micrometers pitch and 70 micrometers width, align with five multiprobes setup in our laboratory. The devices are designed for various types, such as plain (P) and phonon engineered (PE) membranes, in both p and n-type doped versions, and different membranes geometries, as shown in Table 1.

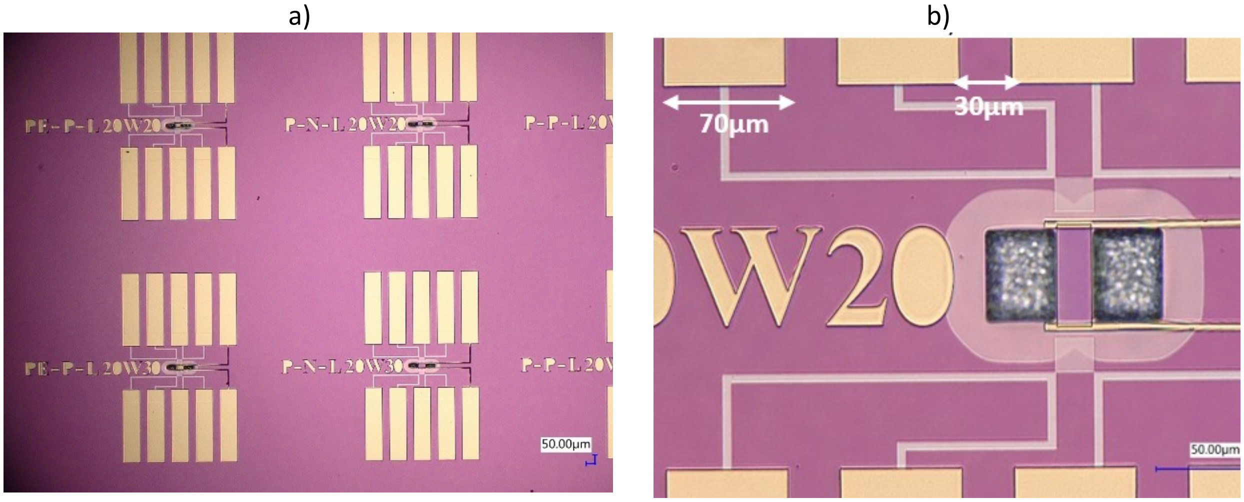
a) b)

Figure 1: The microscope images showcase a) the fabricated Seebeck coefficient measurement device, b) a close-up view of the Si suspended membrane within the Seebeck coefficient measurement device.

Table 1: This table describes the breakdown of all 48 samples with their specific width and length. Of these 48, there were 24 n-type samples indicated in orange; the other 24 were p-type indicated in blue.

	Width (μm)											
Length (μm)	10				20				30			
20	P		PE		P		PE		P		PE	
	n	p	🟧	🟦	🟧	🟦	🟧	🟦	🟧	🟦	🟧	🟦
60	P		PE		P		PE		P		PE	
	🟧	🟦	🟧	🟦	🟧	🟦	🟧	🟦	🟧	🟦	🟧	🟦
100	P		PE		P		PE		P		PE	
	🟧	🟦	🟧	🟦	🟧	🟦	🟧	🟦	🟧	🟦	🟧	🟦
140	P		PE		P		PE		P		PE	
	🟧	🟦	🟧	🟦	🟧	🟦	🟧	🟦	🟧	🟦	🟧	🟦

2. Pt heater serpentine calibration:

The characterizations are performed using a four-probe DC point probes measurement setup. This setup involves connecting the probes to an HP/Agilent 4155C semiconductor parameter analyzer, which serves as an accurate voltage source and current or voltage measurement unit. The HP4155C includes four source monitor units (SMU), capable of functioning as voltage source-current measurement units or current source-voltage measurement units. Additionally, it has two voltage measurement units (VMU) dedicated solely to voltage measurement and two voltage source units (VSU). In our measurements, the SMUs are utilized as voltage source-current measurement units, while the VMUs are used for voltage measurements. This is because the VMUs provide enhanced voltage measurement accuracy, with a precision of ±0.2μV compared to ±2μV and ±1nA for the SMUs. The VMUs are specifically employed for potential difference measurements between two points.

The device under test is voltage biased through the SMUs on two contacts. The potential difference induced by the current from the voltage-biased contacts is measured using the VMUs on the other two contacts. This configuration allows us to determine the central Pt serpentine heater's properties without considering the resistance of the pads. Figure 2 provides a comprehensive overview of the measurement platform and its components; a) The measurement platform is depicted, showcasing the setup used for characterizations. b) A close-up view is presented, highlighting the precise positioning of the probes on the sample. c) The figure displays the probes' positioning in the layout, illustrating their specific arrangement on the device. d) The electrical circuit analogy of the Pt heater calibration is also included, outlining the circuitry and connections involved in this process. These visual representations provide a comprehensive overview of the Pt heater calibration process, including the measurement setup, equipment, probe positioning, and electrical circuitry involved.

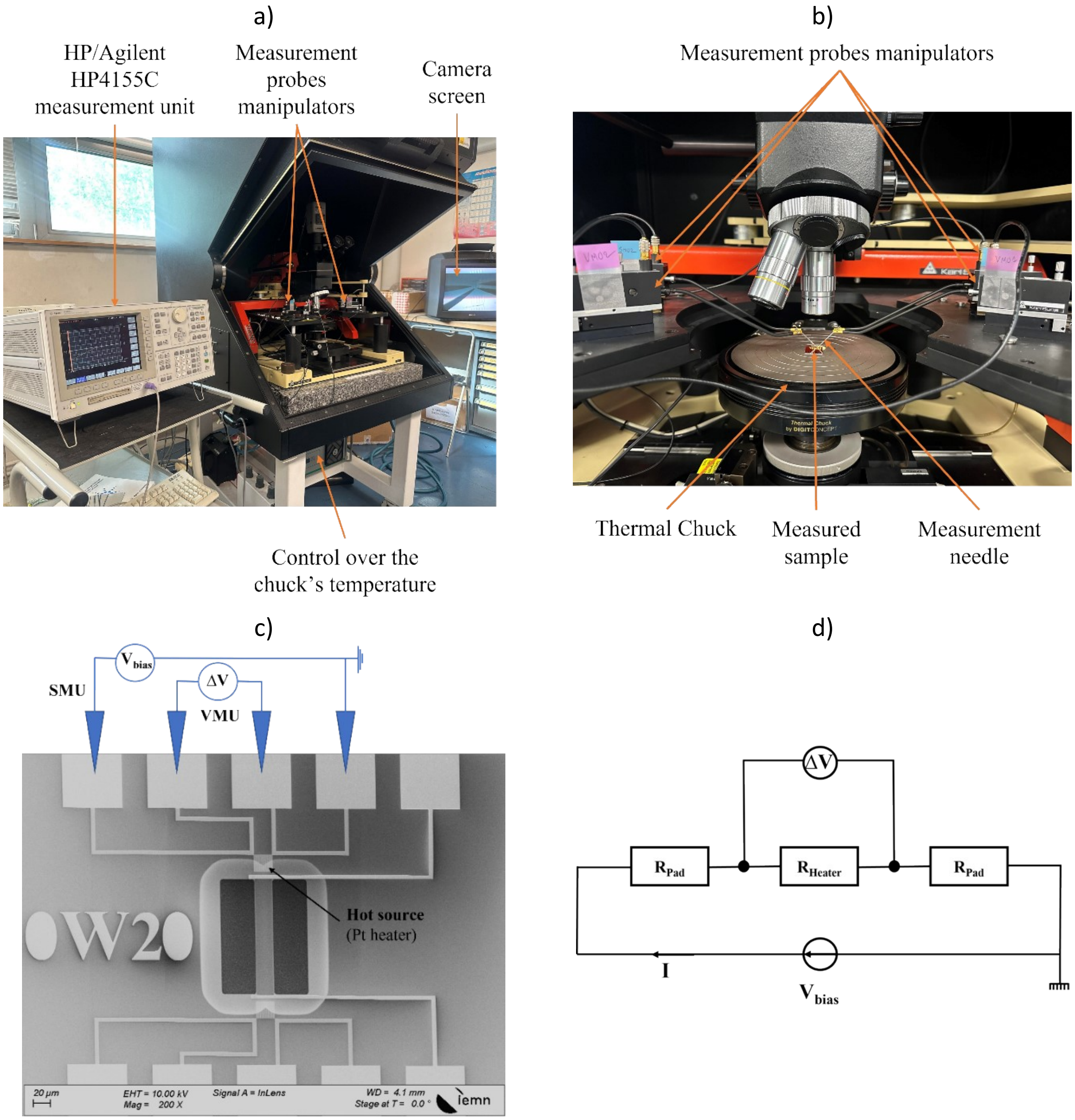

Figure 2: Pt heater calibration. (a) Measurement platform showcasing the setup used for characterizations. (b) Close-up view of the measurement set-up. (c) Probes' positioning in the Seebeck coefficient measurement device. (d) Electrical circuit analogy of the Pt heater calibration.

The measurement protocol for determining the Pt temperature coefficient of resistance (TCR) follows the procedure described above. The chuck's temperature is varied from ambient (23°C) to approximately 45°C, while a range of voltages (-10mV, 0.1mV, 10mV) is applied to the heaters. These voltage levels are intentionally kept at a modest range to prevent notable Joule effect-induced self-heating. This approach allows us to observe the effect of temperature variation on the Pt electrical resistance, as illustrated in Figure 2(c).

As expected, the electrical resistance of Pt exhibits a linear increase with the temperature of the chuck, as illustrated in Figure 3, in accordance with Equation 1. By applying this equation to the measured resistance values obtained from the three devices, the TCR α_i (where 'i' represents the device number) of each device is determined based on the fitting equation correlating the electrical resistance and the chuck's temperature (Equation 2). The average TCR (α) value is calculated from the three measured α_i values (Equation 4). To estimate the uncertainty or error in the calculated TCR (α) value, the error propagation calculation method is employed. This method involves propagating the uncertainties associated with the measured resistance values and the temperature readings to determine the overall error in the TCR (α) calculation. This approach enables us to consider measurement errors and provide a more dependable estimation of the TCR (α_i) values for the Pt heaters in the three devices. Considering that the final estimation of the TCR (α) is obtained through the fitting equation, we can propagate the $\Delta\alpha_i$ error using the Equation 3. The approximate value of the final error $\Delta\alpha$ is calculated using Equation 5 and is determined to be around 2%.

$$R_{Pti}(T) = a_i + b_i \Delta T$$

Equation 1

With a_i and b_i being respectively the intercept and slope of the fitting equation of each device.

$$\alpha_i = b_i / a_i$$

Equation 2

$$\Delta\alpha_i = \sqrt{\left(\frac{\partial \alpha_i}{\partial b_i}\Delta b_i\right)^2 + \left(\frac{\partial \alpha_i}{\partial a_i}\Delta a_i\right)^2}$$

Equation 3

With Δa_i represents the error in the intercept, while Δb_i represents the error in the slope of the fitting equation for each device, as determined using Origin software.

$$\alpha = \frac{\sum_{i=1}^{n} \alpha_i}{n}$$

Equation 4

$$\Delta\alpha = \sqrt{\sum_{i=1}^{n} \left(\frac{\partial \alpha}{\partial \alpha_i}\Delta \alpha_i\right)^2}$$

Equation 5

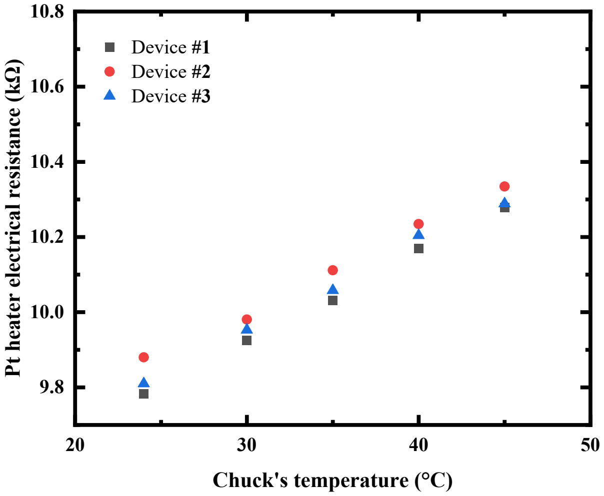

Figure 3: Pt electrical resistance variation with the chuck's temperature for three different devices.

The calculated TCR (α) is 2.495.10^{-3} K^{-1} ± 2% K^{-1} and will be used as a common TCR to determine the temperature difference in all devices. Since all the measured devices are located on the same chip and were subjected to the same process, it can be assumed that the Pt TCR of the demonstrators is equal or at least close (taking into account measurement errors related to the dispersion of one device to another on the wafer.).

3. Absorption estimation:

The RCWA (Rigorous Coupled-Wave Analysis) method is employed to determine the absorption coefficients of both plain membranes and patterned membranes. This method is based on the principles of wave optics and provides a rigorous solution for the interaction of electromagnetic waves with periodic structures. In RCWA, the incident electromagnetic field is decomposed into its constituent plane waves, and the diffraction and scattering phenomena are taken into account by solving Maxwell's equations. By analyzing the transmission and reflection coefficients of these plane waves, the absorption coefficients of the membranes can be calculated.

Figure 4 illustrates the absorption coefficient of plain membranes as a function of membrane thickness (Figure 4-a) using the RCWA method. Additionally, the absorption coefficient of a patterned membrane with a thickness of 60nm and a pitch of 100nm is shown as a function of the holes' diameter (Figure 4-b). The refractive index used in these calculations is obtained from Palik [112](n = 4.463 + i*0.0367).

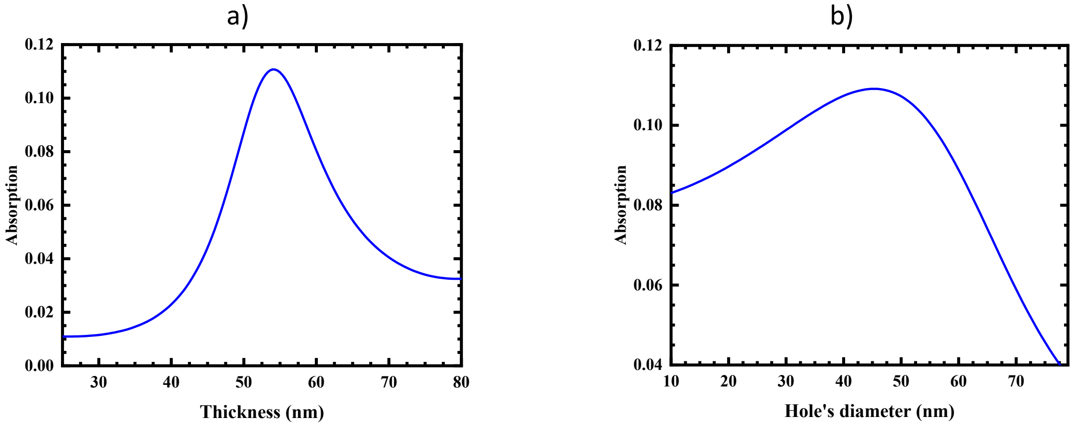

*Figure 4 : RCWA absorption coefficient as a function of (a) thickness of plain membranes and (b) hole's diameter of a 60nm thick patterned membrane with a 100nm pitch. The calculations are based on the refractive index obtained from Palik (n=4.463+ i*0.0367).*

In order to determine the diameters of our patterned membranes, Scanning Electron Microscopy (SEM) images were analyzed, as shown in Figure 5. The diameter of the white shell rim around the holes corresponds to the largest diameter of the hole (top diameter), while the diameter of the dark area represents the bottom hole diameter. For this study, the averaged diameter/radius, calculated by averaging the top- and bottom-hole diameters, was used as a structural characteristic in the analysis of experimental data. The average diameter of our membrane is determined to be 45.95nm. As depicted in Figure 4-b, the absorption of a patterned membrane with diameters ranging from 45nm to 50nm exhibits similar behavior.

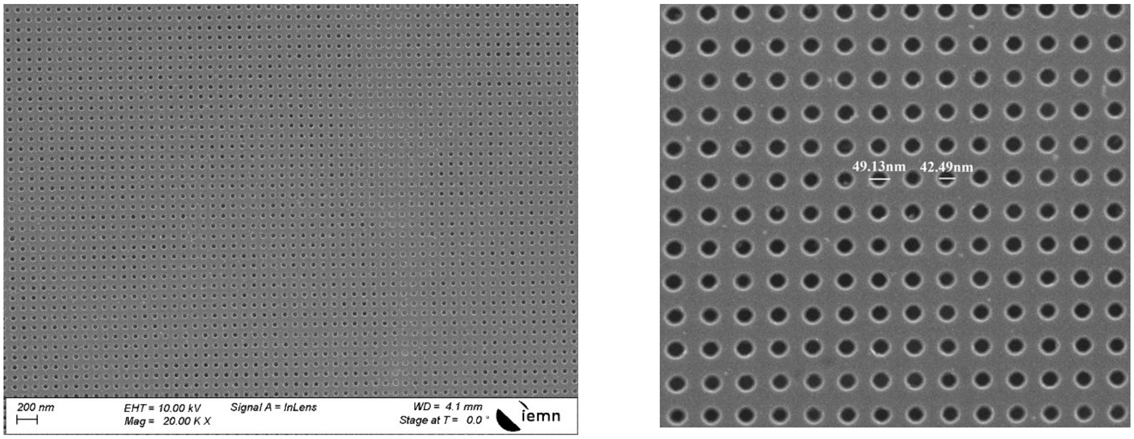

Figure 5: Scanning Electron Microscopy image of periodic patterned nano-holes in silicon.

4. Finite Element Modelling

The crucial aspect of the device geometry that significantly impacts heat propagation compared to the simple slab case is the presence of the SOI "wings." These wings are formed due to etching around the cavity, as depicted in Figure 6-a. They can be considered as extensions of the membrane. The width of the SOI wing, which is a critical parameter, has been determined through SEM analysis, as illustrated in Figure 6-b, and is measured to be 20µm. Additionally, it's important to consider also the SiN remaining on the sides of the membranes and on top of the wings. The width of the SiN on the membrane's sides is 625nm, and its thermal conductivity is 1.55W/mK. This dimension plays a crucial role in determining the heat transfer characteristics and should be taken into account for accurate modeling and analysis of the thermal behavior in the device.

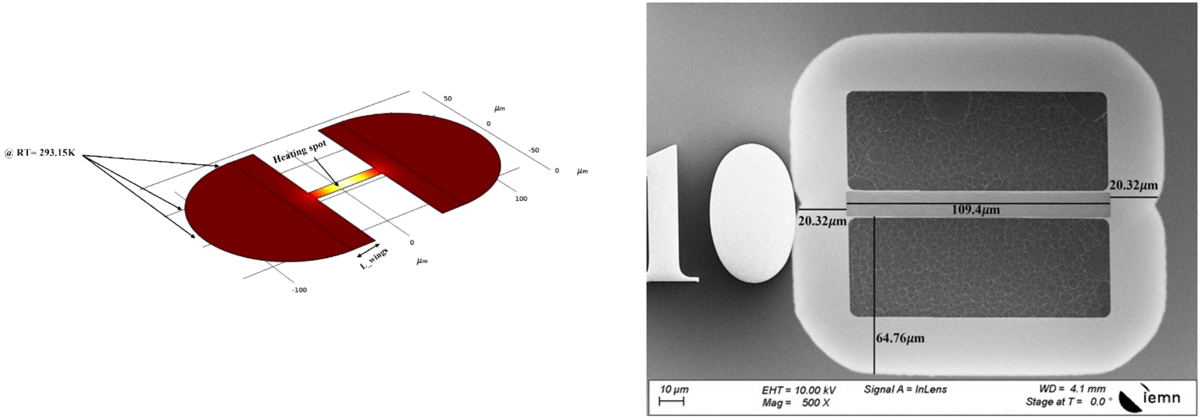
a)

b)

Figure 6: a) COMSOL model for thermal conductivity fitting using experiment geometry and Finite Element Model analyses for heat transfer. b) Scanning Electron Microscopy image of the suspended membrane, showcasing the width of the created wings.

5. Error analysis

We provide below a table that summa s t ro ysi ou nventional error propagation calculation. The typical error ran s s w s sin w. This can be explained by three facts:

i) The Seebeck coefficient is obt ecl eal ng e d curves. These curves are almost perfectly linear (Figure 6 in the article dr a ro ler agnitude 1 µV/K)

ii) The electrical conductivity me rer err low der agnitude 1%)

iii) The thermal conductivity mea em pro to ite urate. We estimated the error to be below 1 W/m/K as can be seen on re the le.

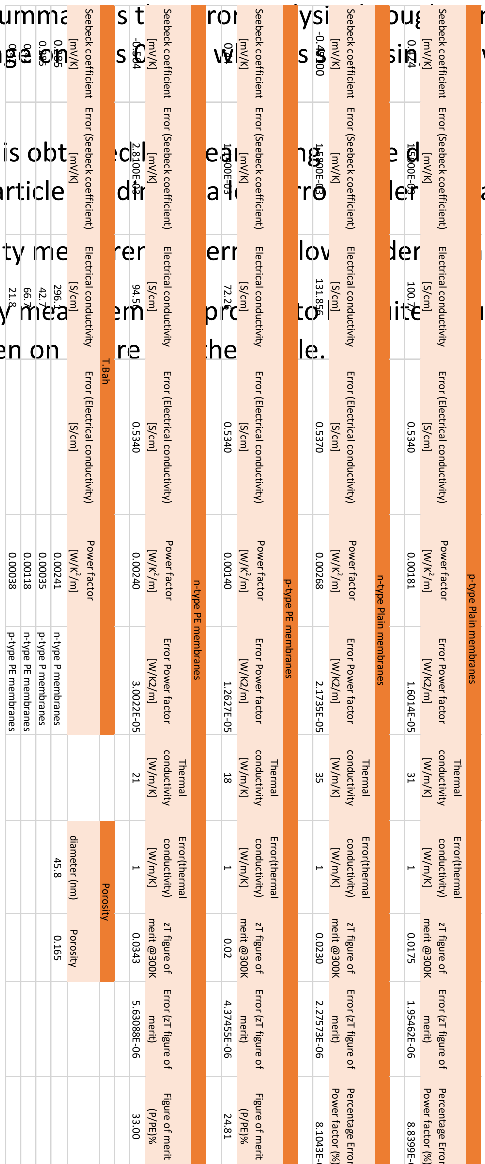

p-type Plain membranes										
Seebeck coefficient [mV/K]	Error (Seebeck coefficient) [mV/K]	Electrical conductivity [S/cm]	Error (Electrical conductivity) [S/cm]	Power factor [W/K^2/m]	Error Power factor [W/K2/m]	Thermal conductivity [W/m/K]	Error(thermal conductivity) [W/m/K]	zT figure of merit @300K	Error (zT figure of merit)	Percentage Erro Power factor (%
0.424	1.5000E-03	100.77	0.5340	0.00181	1.6014E-05	31	1	0.0175	1.95462E-06	8.8399E-
n-type Plain membranes										
Seebeck coefficient [mV/K]	Error (Seebeck coefficient) [mV/K]	Electrical conductivity [S/cm]	Error (Electrical conductivity) [S/cm]	Power factor [W/K^2/m]	Error Power factor [W/K2/m]	Thermal conductivity [W/m/K]	Error(thermal conductivity) [W/m/K]	zT figure of merit @300K	Error (zT figure of merit)	Percentage Erro Power factor (%
-0.45100	1.5800E-03	131.856	0.5370	0.00268	2.1735E-05	35	1	0.0230	2.27573E-06	8.1043E-
p-type PE membranes										
Seebeck coefficient [mV/K]	Error (Seebeck coefficient) [mV/K]	Electrical conductivity [S/cm]	Error (Electrical conductivity) [S/cm]	Power factor [W/K^2/m]	Error Power factor [W/K2/m]	Thermal conductivity [W/m/K]	Error(thermal conductivity) [W/m/K]	zT figure of merit @300K	Error (zT figure of merit)	Figure of merit (P/PE)%
0.44	1.1400E-03	72.26	0.5340	0.00140	1.2627E-05	18	1	0.02	4.37455E-06	24.81
n-type PE membranes										
Seebeck coefficient [mV/K]	Error (Seebeck coefficient) [mV/K]	Electrical conductivity [S/cm]	Error (Electrical conductivity) [S/cm]	Power factor [W/K^2/m]	Error Power factor [W/K2/m]	Thermal conductivity [W/m/K]	Error(thermal conductivity) [W/m/K]	zT figure of merit @300K	Error (zT figure of merit)	Figure of merit (P/PE)%
-0.504	2.8100E-03	94.56	0.5340	0.00240	3.0022E-05	21	1	0.0343	5.63088E-06	33.00
T.Bah							**Porosity**			
Seebeck coefficient [mV/K]	Error (Seebeck coefficient) [mV/K]	Electrical conductivity [S/cm]	Error (Electrical conductivity) [S/cm]	Power factor [W/K^2/m]			diameter (nm)	Porosity		
0.285		296.1		0.00241	n-type P membranes		45.8	0.165		
0.285		42.7		0.00035	p-type P membranes					
0.42		66.7		0.00118	n-type PE membranes					
0.42		21.8		0.00038	p-type PE membranes					